Eur. Phys. J. C 16, 541–546 (2000)
Digital Object Identifier (DOI) 10.1007/s100520000438

THE EUROPEAN
PHYSICAL JOURNAL C

$\gamma\gamma \to t\bar{c} + c\bar{t}$ in a supersymmetric theory with explicit R-parity violation*

Z.H. Yu[1,3], H. Pietschmann[1], W.G. Ma[2,3], L. Han[3], Y. Jiang[3]

[1] Institut für Theoretische Physik, Universität Wien, 1090 Vienna, Austria
[2] CCAST (World Laboratory), P.O. Box 8730, Beijing 100080, P.R. China
[3] Department of Modern Physics, University of Science and Technology of China (USTC), Hefei, Anhui 230027, P.R. China

Received: 20 September 1999 / Revised version: 6 May 2000 /
Published online: 6 July 2000 – © Springer-Verlag 2000

Abstract. We study the process $\gamma\gamma \to t\bar{c} + c\bar{t}$ in a $R_{\rm p}$-violating supersymmetric model with the effects of both B- and L-violating interactions. The calculation shows that it is possible to detect a $R_{\rm p}$-violating signal at the Linear Collider. Information about the B-violating interaction in this model could be obtained with a very clean background, if we take the present upper bounds for the parameters in the supersymmetric $\not{R}_{\rm p}$ interactions. Even if we cannot detect a signal of $\not{R}_{\rm p}$ in the experiment, we may get more stringent constraints on the heavy-flavor $\not{R}_{\rm p}$ couplings.

1 Introduction

The minimal supersymmetric model (MSSM) [1] is one of the most interesting extensions of the standard model (SM) and is considered as the most favorable model beyond SM. Thus, it is interesting to confirm whether R-parity ($R_{\rm p}$), which is introduced to guarantee the B and L conservation automatically, is conserved in the supersymmetric extension of the SM [2]. Because of the lack of credible theoretical arguments and experimental tests for $R_{\rm p}$ conservation, we can say that the $R_{\rm p}$ violation ($\not{R}_{\rm p}$) would be equally well motivated in the supersymmetric extension of the SM [3]. Since in the $R_{\rm p}$-violation models supersymmetry particles can be singly produced and neutrinos would get masses and mixing [4], it is a significant source of new physics. Especially after the first signals of neutrino oscillations from atmospheric neutrinos were observed in Super-Kamiokande [5] and an anomaly was detected in HERA e^+p deep inelastic scattering (DIS) [6], $R_{\rm p}$ violation may be a good candidate to explain those experimental results.

In the last few years, many efforts were made to find $\not{R}_{\rm p}$ interactions in experiments. Unfortunately, up to now we have only some upper limits on the $\not{R}_{\rm p}$ parameters, such as the B-violating $\not{R}_{\rm p}$ parameter ($\lambda^{''}$) and the L-violating $\not{R}_{\rm p}$ parameters (λ and $\lambda^{'}$) [4,7]; results are collected in [8] (the parameters will be defined clearly in the following section). Therefore, trying to find the signal of $R_{\rm p}$ violation or getting more stringent constraints on the parameters in future experiments is a promising task. Possible ways to find a $R_{\rm p}$-violation signal can be detecting odd-number supersymmetric particle interactions as a direct signal or testing discrepancies between the predictions of $R_{\rm p}$-conservation models and $R_{\rm p}$-violation models in the experiments, this giving indirect information.

In our paper we will consider the process $e^+e^- \to \gamma\gamma \to t\bar{c} + c\bar{t}$ in the future Linear Collider (LC). This rare process, which is suppressed by the GIM mechanism in the standard model [9], may be a good window to open new physics. In [10], it was pointed out that anomalous $t\bar{q}\gamma$ coupling admitted by present experimental results may be much larger than the prediction of SM. Thus, $R_{\rm p}$ violation can be a significant source of this anomalous coupling. Although small values of $\lambda^{'}$ and $\lambda^{''}$ in $\not{R}_{\rm p}$ theory would suppress this process, the present upper bounds on the $\not{R}_{\rm p}$ parameters still admit experimental observation ($\lambda^{'}$ and $\lambda^{"}$ can be of order 1 when they involve heavy flavors, which is reasonable with the assumption of family symmetry [11]). So we can hope that this process allows for detection of $R_{\rm p}$ violation within the present parameter upper limits.

With the advent of new collider techniques, we can produce highly coherent laser beams being back-scattered with a high luminosity and efficiency at the e^+e^- colliders [12]. The $\gamma\gamma$ collisions give us a very clean environment to study the $t\bar{c}$ (or $c\bar{t}$) production. The effects of L-violating parameters in e^+e^- collisions have been studied [7], but only little attention was paid to the B-violating parameters [13]. The process considered here can give us an opportunity to detect the B-violating parameter $\lambda^{''}$ in a very

* Supported in part by the Committee of the National Natural Science Foundation of China and Project IV.B.12 of the scientific and technological cooperation agreement between China and Austria

clean environment. We can also get information on the parameter λ' from the process, especially for heavy flavors, which are only weakly constrained by the present data.

Even without $R_{\rm p}$ violation, there are flavor-changing mechanisms [14] in the MSSM, e.g. squark mixing. Therefore, $R_{\rm p}$ violation in $\gamma\gamma \to t\bar{c} + c\bar{t}$ can only be established if it exceeds the value of these other mechanisms. Fortunately, in most models with universal SUSY breaking, those contributions are small (for details see [14]). Hence throughout our paper we shall assume that they are suppressed.

Other possible competing mechanisms, such as the two-Higgs-doublet model (THDM), was considered by Atwood et al. [15] and Jiang et al. [15]. The results showed that the cross section would be much smaller assuming the masses of the higgses to be far from the c.m. energy of the colliders, so we can distinguish them easily from R_p-violation interactions.

In this work we concentrate on the process $e^+e^- \to \gamma\gamma \to t\bar{c} + c\bar{t}$ in the R-parity violating supersymmetric theory. In Sect. 2, we give the supersymmetric $\not{R}_{\rm p}$ interactions. In Sect. 3 we give the analytical calculation of $\gamma\gamma \to t\bar{c} + c\bar{t}$. In Sect. 4 the numerical results of the process $e^+e^- \to \gamma\gamma \to t\bar{c} + c\bar{t}$ are presented. The conclusion is given in Sect. 5 and some details of the expressions are listed in the Appendix.

2 R-parity violation ($\not{R}_{\rm p}$) in MSSM

All renormalizable supersymmetric $\not{R}_{\rm p}$ interactions can be introduced in the superpotential [8]:

$$
\begin{aligned}
W_{\not{R}_{\rm p}} &= \frac{1}{2}\lambda_{[ij]k} L_i \cdot L_j \bar{E}_k + \lambda'_{ijk} L_i \cdot Q_j \bar{D}_k \\
&+ \frac{1}{2}\lambda''_{i[jk]} \bar{U}_i \bar{D}_j \bar{D}_k + \epsilon_i L_i H_u, \qquad (2.1)
\end{aligned}
$$

where L_i, Q_i and H_u are SU(2) doublets containing lepton, quark and Higgs superfields, respectively; $\bar{E}_j$ ($\bar{D}_j$, $\bar{U}_j$) are the singlets of the lepton (down-quark and up-quark), and i, j, k are generation indices. Square brackets on them denote antisymmetry in the bracketed indices.

We ignored the last term in (2.1), which will introduce mixing of leptons and higgses, since its effects are rather small in our process [4,16]. So we have 9 λ-type, 27 λ'-type and 9 λ''-type independent parameters left. The Lagrangian density of $\not{R}_{\rm p}$ is given as follows (to lowest order of λ):

$$
\begin{aligned}
L_{\not{R}_{\rm p}} &= L^{\lambda}_{\not{R}_{\rm p}} + L^{\lambda'}_{\not{R}_{\rm p}} + L^{\lambda''}_{\not{R}_{\rm p}} \qquad (2.2)\\
L^{\lambda}_{\not{R}_{\rm p}} &= \lambda_{[ij]k}[\tilde{\nu}_{i{\rm L}}\bar{e}_{k{\rm R}}e_{j{\rm L}} + \tilde{e}_{j{\rm L}}\bar{e}_{k{\rm R}}\nu_{i{\rm L}} + \tilde{e}^*_{k{\rm R}}\overline{\nu^c_{i{\rm L}}}e_{j{\rm L}} \\
&- \tilde{\nu}_{j{\rm L}}\bar{e}_{k{\rm R}}e_{i{\rm L}} - \tilde{e}_{i{\rm L}}\bar{e}_{k{\rm R}}\nu_{j{\rm L}} - \tilde{e}^*_{k{\rm R}}\overline{\nu^c_{j{\rm L}}}e_{i{\rm L}}] + {\rm h.c.} \\
L^{\lambda'}_{\not{R}_{\rm p}} &= \lambda'_{ijk}[\tilde{\nu}_{i{\rm L}}\bar{d}_{k{\rm R}}d_{j{\rm L}} + \tilde{d}_{j{\rm L}}\bar{d}_{k{\rm R}}\nu_{i{\rm L}} + \tilde{d}^*_{k{\rm R}}\overline{\nu^c_{i{\rm L}}}d_{j{\rm L}} \\
&- \tilde{e}_{i{\rm L}}\bar{d}_{k{\rm R}}u_{j{\rm L}} - \tilde{u}_{j{\rm L}}\bar{d}_{k{\rm R}}e_{j{\rm L}} - \tilde{d}^*_{k{\rm R}}\overline{e^c_{i{\rm L}}}u_{j{\rm L}}] + {\rm h.c.} \\
L^{\lambda''}_{\not{R}_{\rm p}} &= \lambda''_{i[jk]}\epsilon_{\alpha\beta\gamma}[\tilde{u}^*_{i{\rm R}\alpha}\bar{d}_{k{\rm R}\beta}d^c_{j{\rm R}\gamma} + \tilde{d}^*_{j{\rm R}\beta}\bar{u}_{i{\rm R}\alpha}d^c_{k{\rm R}\gamma} \\
&+ \tilde{d}^*_{k{\rm R}\gamma}\bar{u}_{i{\rm R}\alpha}d^c_{j{\rm R}\beta}] + {\rm h.c.} \qquad (2.3)
\end{aligned}
$$

The proton lifetime suppresses the possibility of both B violation and L violation, leading to the constraints [8]:

$$
|(\lambda \text{ or } \lambda')\lambda''| < 10^{-10}\left(\frac{\tilde{m}}{100\,{\rm GeV}}\right)^2 \qquad (2.4)
$$

where $\tilde{m}$ is the mass of superquark or superlepton. Therefore, we consider the contributions from $L^{\lambda'}_{\not{R}_{\rm p}}$ and $L^{\lambda''}_{\not{R}_{\rm p}}$ separately. Although the individual parameters λ, λ' and λ'' should be typically less than 10^{-1}–$10^{-2}(\tilde{m}/(100\,{\rm GeV}))^2$ [8], we can expect the parameters involving heavy flavors to be much larger in analogy with the Yukawa couplings in the MSSM [11]. Since the constraints on such parameters from present experimental data are rather weak, testing $\not{R}_{\rm p}$ at high energy is still very important.

3 Calculations

In the following calculations we assume the parameters λ' and λ'' to be real. One-loop corrections (as shown in Fig. 1) of $\gamma(p_3)\gamma(p_4) \to t(p1)\bar{c}(p2)$ can be split into the following components:

$$
M = \delta M_s + \delta M_v + \delta M_b, \qquad (3.1)
$$

where $\delta M_{\rm s}$, $\delta M_{\rm v}$ and $\delta M_{\rm b}$ are the one-loop amplitudes corresponding to the self-energy, vertex, and box correction diagrams, respectively. We find that the amplitudes are proportional to the products $\lambda'_{i2j}\lambda'_{i3j}$ $(i, j = 1, 2, 3)$ (Fig. 1a.1-2, Fig. 1b.1-4 and Fig. 1c.1-8) and $\lambda''_{2ij}\lambda''_{3ij}$ $(i, j = 1, 2, 3)$ (Fig. 1a.3, Fig. 1b.5-6 and Fig. 1c.9-12); thus, it is possible to detect $\not{R}_{\rm p}$ signals or get much stronger constraints on those parameters by measuring this process in future LC experiments.

We define the Mandelstam variables as usual:

$$
\begin{aligned}
\hat{s} &= (p_1 + p_2)^2 = (p_3 + p_4)^2, \qquad (3.2)\\
\hat{t} &= (p_1 - p_3)^2 = (p_4 - p_2)^2, \qquad (3.3)\\
\hat{u} &= (p_1 - p_4)^2 = (p_3 - p_2)^2. \qquad (3.4)
\end{aligned}
$$

The $t\bar{c} + c\bar{t}$ productions via $\gamma\gamma$ fusion obtains contributions only from one-loop Feynman diagrams at the lowest order. Since the proper vertex counterterm should cancel with the counterterms of the external leg diagrams in this case, we do not need to deal with the ultraviolet divergence. Thus we simply sum over all (unrenormalized) reducible and irreducible diagrams and the result is finite and gauge invariant. In the Appendix we will give the details of the amplitudes. Similarly, we can get the amplitude for the subprocess $\gamma\gamma \to c\bar{t}$. Collecting all terms in (3.1), we obtain the total cross section for the subprocess $\gamma\gamma \to t\bar{c} + c\bar{t}$:

$$
\hat{\sigma}(\hat{s}) = \frac{2N_c}{16\pi\hat{s}^2}\int_{\hat{t}^-}^{\hat{t}^+} {\rm d}\hat{t}\,\overline{\sum_{\rm spins}}[|M|^2], \qquad (3.5)
$$

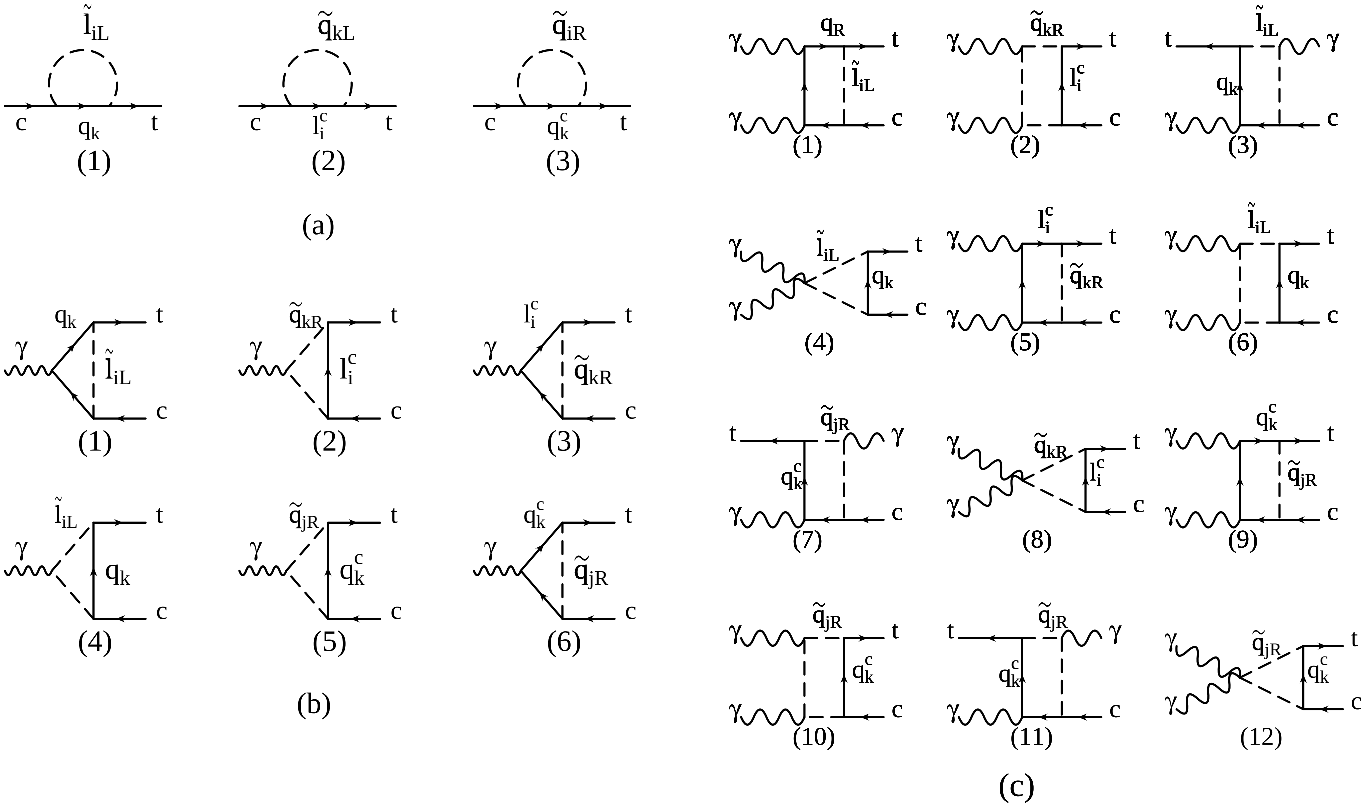

Fig. 1a–c. Feynman diagrams of $\gamma\gamma \to t\bar{c}$ subprocess. **a** Self-energy diagrams, **b** vertex diagrams, **c** box diagrams (only t-channel). Dashed lines represent sleptons and squarks

where $\hat{t}^{\pm} = (1/2)\left[(m_t^2 + m_c^2 - \hat{s}) \pm (\hat{s}^2 + m_t^4 + m_c^4 - 2\hat{s} * m_t^2 - 2\hat{s} * m_c^2 - 2m_t^2 * m_c^2)^{1/2}\right]$, the color factor is $N_c = 3$ and the bar over summation means averaging over the initial spins. In order to get the observable results in the measurements of $t\bar{c} + \bar{t}c$ production via $\gamma\gamma$ fusion in the e^+e^- collider, we need to fold the cross section of $\gamma\gamma \to t\bar{c} + c\bar{t}$ with the photon luminosity:

$$\sigma(s) = \int_{(m_t+m_c)/\sqrt{s}}^{x_{\max}} \mathrm{d}z \frac{\mathrm{d}L_{\gamma\gamma}}{\mathrm{d}z} \hat{\sigma}(\hat{s}), \qquad (3.6)$$

where $\hat{s} = z^2 s$, $s^{1/2}$ and $\hat{s}^{1/2}$ are the e^+e^- and $\gamma\gamma$ CMS energies, respectively, and $\mathrm{d}L_{\gamma\gamma}/\mathrm{d}z)$ is the photon luminosity, which is defined as [12]

$$\frac{\mathrm{d}L_{\gamma\gamma}}{\mathrm{d}z} = 2z \int_{z^2/x_{\max}}^{x_{\max}} \frac{\mathrm{d}x}{x} F_{\gamma/e}(x) F_{\gamma/e}(z^2/x). \qquad (3.7)$$

The energy spectrum of the back-scattered photon is given by [12].

$$F_{\gamma/e}(x) = \frac{1}{D(\xi)}\left[1 - x + \frac{1}{1-x} - \frac{4x}{\xi(1-x)} + \frac{4x^2}{\xi^2(1-x)^2}\right]. \qquad (3.8)$$

Taking the parameters of [17], we have $\xi = 4.8$, $x_{\max} = 0.83$ and $D(\xi) = 1.8$.

4 Numerical results

In the numerical calculations, we assume $m_{\tilde{q}} = m_{\tilde{l}}$ and consider the effects from $L_{\not R_{\mathrm{P}}}^{\lambda'}$ and $L_{\not R_{\mathrm{P}}}^{\lambda''}$ separately. This will be no loss of generality and the results could be kept in the bounds of realistic models of supersymmetry.

For the B-violating parameter $\lambda''_{2ij}\lambda''_{3ij} (i, j = 1\text{–}3)$, the upper bounds of λ''_{223} and λ''_{323} dominate all others, so we will neglect all other λ'' terms. For the L-violating parameter $\lambda'_{i2j}\lambda'_{i3j}$ $(i, j = 1\text{–}3)$, we neglect all parameters except for λ'_{323} and λ'_{333}.

In Fig. 2, we show the cross section of $e^+e^- \to \gamma\gamma \to t\bar{c} + c\bar{t}$ as a function of the c.m. energy of the electron–positron system at the upper bounds of λ'', i.e. $\lambda''_{323}\lambda''_{223} = 0.625$ [4]. We take $m_{\tilde{l}} = m_{\tilde{q}} = 100\,\mathrm{GeV}$ (solid line) and $m_{\tilde{l}} = m_{\tilde{q}} = 150\,\mathrm{GeV}$ (dashed line), respectively. The results show that the cross section can be 0.64 fb for the solid line (0.29 fb for the dashed line) when the c.m. energy ($s^{1/2}$) is equal to 500 GeV. So if the electron–positron integrated luminosity of the LC is $50\,\mathrm{fb}^{-1}$, we can get about 32 events per year when $m_{\tilde{l}} = m_{\tilde{q}} = 100\,\mathrm{GeV}$. Therefore the $\not R_{\mathrm{P}}$ signal could be detected, if λ'' were large enough under the present allowed upper bounds.

In Fig. 3, we plot the cross section of $e^+e^- \to \gamma\gamma \to t\bar{c} + c\bar{t}$ as a function of the c.m. energy of the electron–positron system with the upper bounds of λ', i.e. $\lambda'_{333}\lambda'_{323} = 0.096$; see [4]. We again take $m_{\tilde{l}} = m_{\tilde{q}} = 100\,\mathrm{GeV}$ for

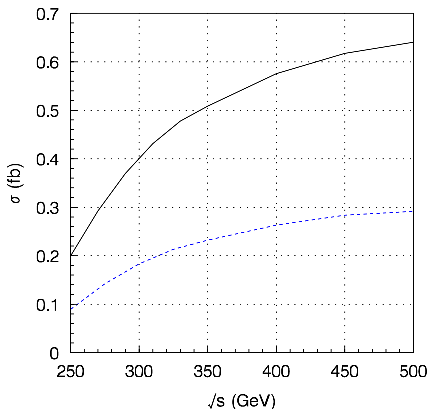

Fig. 2. Cross section of $e^+e^- \to \gamma\gamma \to t\bar{c} + c\bar{t}$ as a function of the c.m. energy $s^{1/2}$ with $\lambda''_{323}\lambda''_{223} = 0.625$. The solid line is for $m_{\tilde{l}} = m_{\tilde{q}} = 100\,\mathrm{GeV}$, and the dashed line for $m_{\tilde{l}} = m_{\tilde{q}} = 150\,\mathrm{GeV}$

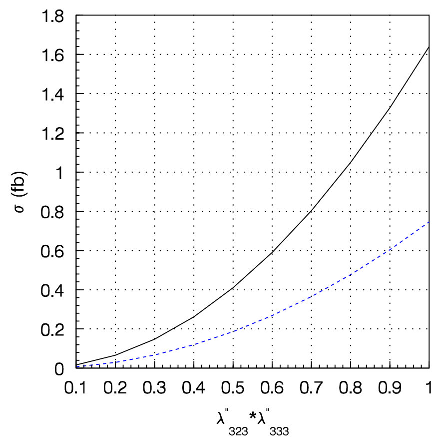

Fig. 4. Cross section of $e^+e^- \to \gamma\gamma \to t\bar{c} + c\bar{t}$ at the c.m. energy $s^{1/2} = 500\,\mathrm{GeV}$ as a function of $\lambda''_{323}\lambda''_{223}$. The solid line for $m_{\tilde{l}} = m_{\tilde{q}} = 100\,\mathrm{GeV}$, and the dashed line for $m_{\tilde{l}} = m_{\tilde{q}} = 150\,\mathrm{GeV}$

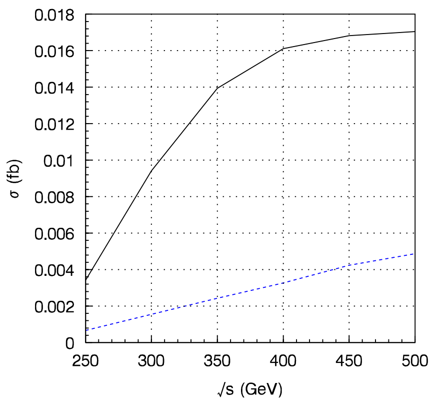

Fig. 3. Cross section of $e^+e^- \to \gamma\gamma \to t\bar{c} + c\bar{t}$ as a function of the c.m. energy $s^{1/2}$ with $\lambda'_{333}\lambda'_{323} = 0.096$. The solid line is for $m_{\tilde{l}} = m_{\tilde{q}} = 100\,\mathrm{GeV}$, and the dashed line for $m_{\tilde{l}} = m_{\tilde{q}} = 150\,\mathrm{GeV}$

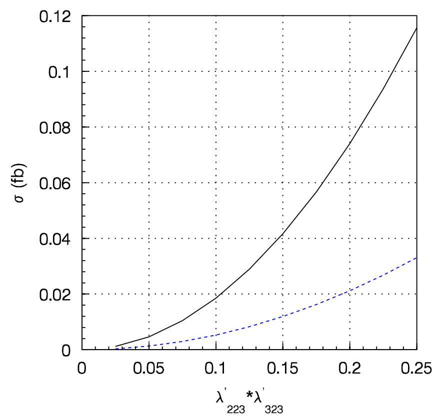

Fig. 5. Cross section of $e^+e^- \to \gamma\gamma \to t\bar{c} + c\bar{t}$ at the c.m. energy $s^{1/2} = 500\,\mathrm{GeV}$ as a function of $\lambda'_{333}\lambda'_{323}$. The solid line is for $m_{\tilde{l}} = m_{\tilde{q}} = 100\,\mathrm{GeV}$, and the dashed line for $m_{\tilde{l}} = m_{\tilde{q}} = 150\,\mathrm{GeV}$

the solid line and $m_{\tilde{l}} = m_{\tilde{q}} = 150\,\mathrm{GeV}$ for the dashed line, respectively. The cross section is much smaller than that of Figure 2. That seems reasonable because the upper limits of λ' from the present data are much smaller than those of λ''. The cross section can be only about 0.017 fb when $s^{1/2} = 500\,\mathrm{GeV}$, which means we can get only 1 event per year at the LC with an integrated luminosity of $50\,\mathrm{fb}^{-1}$. Thus it will be difficult to find the signal of λ' from the process which we discussed.

In order to give more stringent constraints of λ'' in future experiments, we draw the cross section at $s^{1/2} = 500\,\mathrm{GeV}$ as a function of $\lambda''_{223}\lambda''_{323}$ in Fig. 4 (the solid line is for $m_{\tilde{l}} = m_{\tilde{q}} = 100\,\mathrm{GeV}$ and the dashed line for $m_{\tilde{l}} = m_{\tilde{q}} = 150\,\mathrm{GeV}$). When $\lambda''_{223}\lambda''_{323}$ is about 0.1, the cross section will be about 0.02 fb. That corresponds to 1 event per year at the LC. So if we cannot get the signal of $\not{R}_{\mathrm{p}}$ from the experiments, we can set the stronger constraint on λ''_{223} and λ''_{323}, i.e. $\lambda''_{223}\lambda''_{323} \leq 0.1$.

Similarly we draw the relation between the cross section and the parameter product $\lambda'_{323}\lambda'_{333}$ with $s^{1/2} = 500\,\mathrm{GeV}$ in Fig. 5; the solid line is for $m_{\tilde{l}} = m_{\tilde{q}} = 100\,\mathrm{GeV}$ and the dashed line for $m_{\tilde{l}} = m_{\tilde{q}} = 150\,\mathrm{GeV}$.

5 Conclusion

We studied both the subprocess $\gamma\gamma \to t\bar{c} + c\bar{t}$ and the process $e^+e^- \to \gamma\gamma \to t\bar{c} + c\bar{t}$ in one-loop order in an explicit $\not{R}_{\mathrm{p}}$ supersymmetric model. The calculations show that we can test $\not{R}_{\mathrm{p}}$ theory in the future LC experiments if the B-violating couplings (λ''-type) are large enough within the present experimentally admitted range. That means we can detect B-violating interactions in the lepton colliders with a cleaner background. We also consider the effect from L-violating interactions (λ'-type), and conclude that it is very small in this process.

From our calculation, we find that the subprocess $\gamma\gamma \to t\bar{c} + c\bar{t}$ is very helpful in getting information about the B-violating couplings (λ''). That is because the effect of L-violating interactions (λ') is small and can be neglected.

Thus, if we can observe events of this process in the LC, we can conclude that they are from B-violation couplings. Even if we cannot detect any signal from the experiments, we could improve the present upper bounds on $\lambda''_{223}\lambda''_{323}$.

Acknowledgements. The authors would like to thank Prof. H. Stremnitzer for reading the manuscript.

A Loop integrals

We adopt the definitions of two-, three-, four-point one-loop Passarino–Veltman integral functions of [18,19]. The integral functions are defined as follows.

The two-point integrals are

$$\{B_0; B_\mu; B_{\mu\nu}\}(p, m_1, m_2) = \frac{(2\pi\mu)^{4-n}}{\mathrm{i}\pi^2} \int \mathrm{d}^n q \frac{\{1; q_\mu; q_\mu q_\nu\}}{[q^2 - m_1^2][(q+p)^2 - m_2^2]}. \quad (A.1)$$

The function B_μ should be proportional to p_μ:

$$B_\mu(p, m_1, m_2) = p_\mu B_1(p, m_1, m_2). \quad (A.2)$$

Similarly we get

$$B_{\mu\nu} = p_\mu p_\nu B_{21} + g_{\mu\nu} B_{22}. \quad (A.3)$$

We denote $\bar{B}_0 = B_0 - \Delta$, $\bar{B}_1 = B_1 + (1/2)\Delta$ and $\bar{B}_{21} = B_{21} - (1/3)\Delta$, with $\Delta = (2/\epsilon) - \gamma + \log(4\pi)$, $\epsilon = 4 - n$. μ is the scale parameter. The three-point and four-point integrals can be obtained similarly.

The numerical calculation of the vector and tensor loop integral functions can be traced back to the four scalar loop integrals A_0, B_0, C_0 and D_0 in [18,19] and the references therein.

B Self-energy part of the amplitude

The amplitude of the self-energy diagrams δM_s (Fig. 1a) can be decomposed into t-channel terms M_s^t and u-channel terms M_s^u. We will just give the expressions of the t-channel; the u-channel can be obtained from the t-channel by changing t into u and exchanging all indices and arguments of the incoming photons. The amplitude M_s^t can be expressed as

$$\delta M_\mathrm{s}^t = \delta M_\mathrm{s}^{t(a)} + \delta M_\mathrm{s}^{t(b)} + \delta M_\mathrm{s}^{t(c)}, \quad (B.1)$$

where

$$\begin{aligned}
\delta M_\mathrm{s}^{t(a)} &= \frac{-4\pi \mathrm{i}\alpha Q_c Q_t}{(t - m_t^2)(t - m_c^2)} \epsilon^\mu(p_3)\epsilon^\nu(p_4)\bar{u}(p_1)\gamma_\mu \\
&\times (\not{p}_1 - \not{p}_3 + m_t)\,[\Sigma(p_1 - p_3)] \\
&\times (\not{p}_1 - \not{p}_3 + m_c)\gamma_\nu v(p_2), \quad (B.2)\\
\delta M_\mathrm{s}^{t(b)} &= \frac{-4\pi \mathrm{i}\alpha Q_c^2}{(m_t^2 - m_c^2)(t - m_c^2)} \epsilon^\mu(p_3)\epsilon^\nu(p_4)\bar{u}(p_1) \\
&\times \Sigma(p1)(\not{p}_1 + m_c)\gamma_\mu(\not{p}_1 - \not{p}_3 + m_c) \\
&\times \gamma_\nu v(p_2), \quad (B.3)\\
\delta M_\mathrm{s}^{t(c)} &= \frac{-4\pi \mathrm{i}\alpha Q_t^2}{(t - m_t^2)(m_c^2 - m_t^2)} \epsilon^\mu(p_3)\epsilon^\nu(p_4)\bar{u}(p_1) \\
&\times \gamma_\mu(\not{p}_1 - \not{p}_3 + m_t)\gamma_\nu(-\not{p}_2 + m_t) \\
&\times \Sigma(-p2)v(p_2), \quad (B.4)
\end{aligned}$$

where the electric charge of the quark is $Q_c = Q_t = 2/3$, $\alpha = 1/137.04$, and $\Sigma(p)$ is defined as

$$-\mathrm{i}\Sigma(p) = H_\mathrm{L}\not{p}P_\mathrm{L} + H_\mathrm{R}\not{p}P_\mathrm{R} - H_\mathrm{L}^S P_\mathrm{L} - H_\mathrm{R}^S P_\mathrm{R}\delta_{kl}, \quad (B.5)$$

with

$$\begin{aligned}
H_\mathrm{R} &= -\mathrm{i}\Sigma_\mathrm{L}, \quad (B.6)\\
H_\mathrm{R} &= -\mathrm{i}\Sigma_\mathrm{R}, \quad (B.7)\\
H_\mathrm{L}^S &= 0, \quad (B.8)\\
H_\mathrm{R}^S &= 0, \quad (B.9)
\end{aligned}$$

where

$$\begin{aligned}
\Sigma_\mathrm{L} &= -\frac{\mathrm{i}}{16\pi^2}\lambda'_{i2j}\lambda'_{i3j}(B_1[-p, m_{q_j}, m_{\tilde{l}_i}] \\
&+ B_1[-p, m_{l_i}, m_{\tilde{q}_j}]), \quad (B.10)\\
\Sigma_\mathrm{R} &= -\frac{\mathrm{i}C_\mathrm{R}}{16\pi^2}\lambda''_{2jk}\lambda''_{3jk}(B_1[-p, m_{q_j}, m_{\tilde{q}_k}] \\
&+ B_1[-p, m_{q_k}, m_{\tilde{q}_j}]), \quad (B.11)
\end{aligned}$$

where i and j, k are generations of leptons and quarks, respectively, and $C_\mathrm{R} = 2$.

The amplitude from vertex diagrams and box terms can be obtained in a similar way from Fig. 1b,c; however, it is very complex, so we do not express them here. For a hint of its structure, compare with [20]

References

1. H.E. Haber, G.L. Kane, Phys. Rep. **117**, 75 (1985); J.F. Gunion, H.E. Haber, Nucl. Phys. B **272**, 1 (1986)
2. G. Farrar, P. Fayet, Phys. Lett. B **76**, 575 (1978)
3. L.J. Hall, M. Suzuki, Nucl. Phys. B **231**, 419 (1984)
4. C.S. Aulakh, R.N. Mohapatra, Phys. Lett. B **119**, 136 (1982); J. Ellis, G. Gelmini, C. Jarlskog, G.G. Ross, J.W.F. Valle, Phys. Lett. B **150**, 142 (1985); G.G Ross, J.W.F. Valle, Phys. Lett. B **151**, 375 (1985); A. Santamaria, J.W.F. Valle, Phys. Lett. B **195**, 423 (1987)
5. Y. Fukuda et al, Phys. Rev. Lett. **81**, 1562 (1998)
6. C. Adloff et al, Z. Phys. C **74**, 191 (1997); J. Breitweg et al, Z. Phys. C **74**, 207 (1997); J. Butterworth, H. Dreiner, Nucl. Phys. B **397**, 3 (1993)
7. S. Weinberg, Phys. Rev. D **26**, 287 (1982); P. Roy, TIFR/TH/97-60; D.K. Ghosh, S. Raychaudhburi, K. Sridbar, Phys. Lett. B **396**, 177 (1997); K. Agashe, M. Graesser, Phys. Rev. D **54**, 4445 (1996); K. Huitu, J. Maalampi, M. Raidl, A. Santamaria, Phys. Lett. B **430**, 355 (1998); J-H. Jiang, J.G. Kim, J.S. Lee, Phys. Rev. D **55**, 7296 (1997); Phys. Lett. B **408**, 367 (1997); Phys. Rev. D **58**, 035006 (1998); G. Bhattacharyya, D. Choudhury, K. Sridhar, Phys. Lett. B **355**, 193 (1995); J. Ferrandis, Phys. Rev. D **60**, 095012 (1999); M.A. Diaz, J.

Ferrandis, J.C. Romao, J.W.F. Valle, Phys. Lett. B 453; hep-ph/9906343; M.A. Diaz, J. Ferrandis, J.W.F. Valle, hep-ph/9909212; B.C. Allanach, A. Dedes, H.K. Dreiner, Phys. Rev. D **60**, 075014 (1999); S. Bar-Shalom, G. Eilam, J. Wudka, Phys. Rev. D **59**, 035010 (1999); S. Bar-Shalom, G. Eilam, A. Soni, hep-ph/9812518
8. R. Barbier et al., hep-ph/9810232; B. Allanach et al., hep-ph/9906224
9. C.S. Huang et al., Phys. Lett. B **452**, 143 (1999)
10. K.J. Abraham, K. Whisnant, B.-L. Young, Phys. Lett. B **419**, 381 (1998)
11. C.D. Froggatt, H.B. Nielsen, Nucl. Phys. B **147**, 277 (1979)
12. V. Telnov, Nucl. Instrum. Meth. A **294**, 72 (1990); L. Ginzburg, G. Kotkin, H. Spiesbergerm, Fortschr. Phys. **34**, 687 (1986)
13. D.K. Ghosh, R.M. Godbole, S. Raychaudhuri, Z. Phys. C **75**, 357 (1997)
14. S. Dimopoulos, G.F. Giudice, N. Tetradis, Nucl. Phys. B **454**, 59 (1995); F. Gabbiani et al., ROM2F/96/21
15. D. Atwood et al., Phys. Rev. D **53**, 1199 (1996); W-S. Hou, G-L. Lin, Phys. Lett. B **379**, 261 (1996); Y. Jiang, M-l. Zhou, W-G. Ma, L. Han, H. Zhou, M. Han, Phys. Rev. D **57**, 4343 (1998)
16. R. Hempfling, Nucl. Phys. B **478**, 3 (1996); B. Mukhopadhay, S. Roy, Phys. Rev. D **55**, 7020 (1997)
17. K. Cheung, Phys. Rev. D **47**, 3750 (1993); **50**, 1173 (1994)
18. Bernd A. Kniehl, Phys. Rep. **240**, 211 (1994)
19. G. Passarino, M. Veltman, Nucl. Phys. B **160**, 151 (1979)
20. Z-H.Yu, H. Pietschmann, W-G.Ma, L. Han, Y. Jiang, Euro. Phys. C **9**, 463 (1999)